

# Dalton Transactions

Accepted Manuscript



This is an *Accepted Manuscript*, which has been through the Royal Society of Chemistry peer review process and has been accepted for publication.

*Accepted Manuscripts* are published online shortly after acceptance, before technical editing, formatting and proof reading. Using this free service, authors can make their results available to the community, in citable form, before we publish the edited article. We will replace this *Accepted Manuscript* with the edited and formatted *Advance Article* as soon as it is available.

You can find more information about *Accepted Manuscripts* in the [Information for Authors](#).

Please note that technical editing may introduce minor changes to the text and/or graphics, which may alter content. The journal's standard [Terms & Conditions](#) and the [Ethical guidelines](#) still apply. In no event shall the Royal Society of Chemistry be held responsible for any errors or omissions in this *Accepted Manuscript* or any consequences arising from the use of any information it contains.

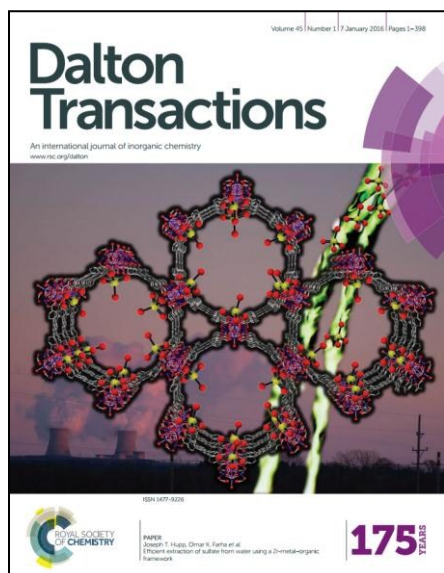
# Dalton Transactions

## Guidelines to Referees

Communications & Papers

The international journal for inorganic, organometallic and bioinorganic chemistry

<http://www.rsc.org/dalton>



**Dalton Transactions** wishes to encourage high quality articles reporting exciting new developments in inorganic chemistry.

For an article to be accepted, it must report new, high-quality research and make a significant contribution to the field.

Manuscripts that describe purely physical, crystallographic or computational studies must include the clear relevance of the work to the broad inorganic chemistry readership of *Dalton Transactions*.

**Communications** must report chemistry of sufficient importance and impact to justify preliminary publication. **Papers** should report more complete studies.

**Dalton Transactions' Impact Factor is 4.19 (2014 Journal Citation Reports®)**

Routine or unnecessarily fragmented work, however competently researched and reported, should not be recommended for publication.

**Thank you very much for your assistance in evaluating this manuscript**

Dr Andrew Shore ([dalton@rsc.org](mailto:dalton@rsc.org))  
Royal Society of Chemistry  
Editor, *Dalton Transactions*

Professor John Arnold  
University of California, Berkeley  
Chair, *Dalton Transactions* Editorial Board

**General Guidance (for further details, see the RSC [Refereeing Procedure and Policy](#))**

*When preparing your report, please:*

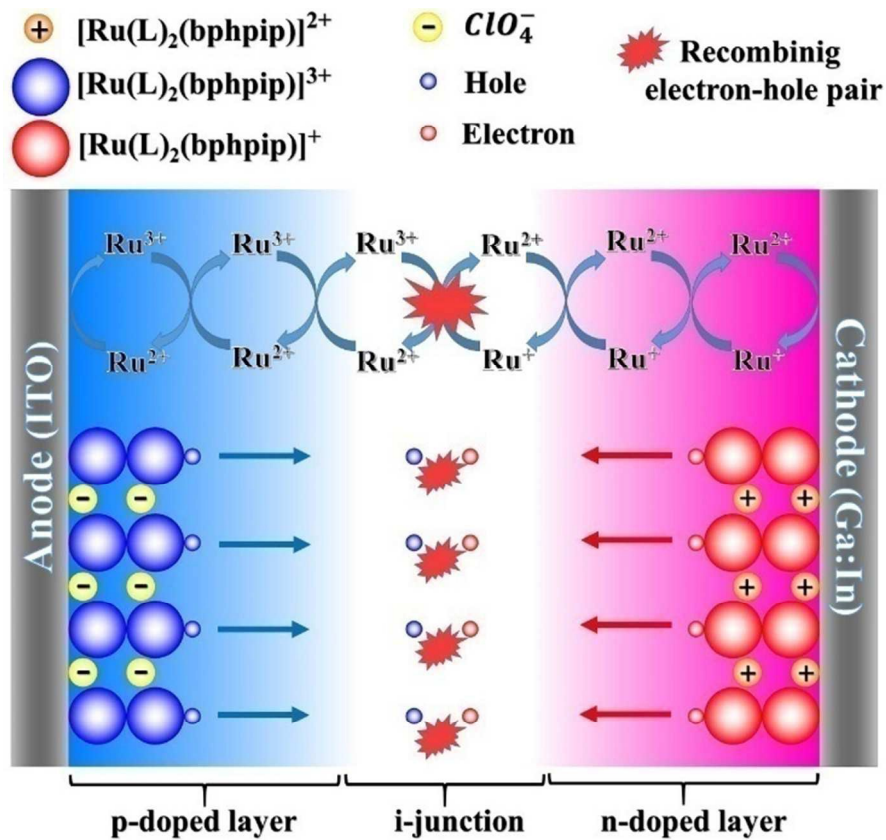
- Comment on the **originality, importance, impact** and **scientific reliability** of the work
- State clearly whether you would like to see the paper accepted or rejected and give detailed comments (with references, as appropriate) that will help both the Editor to make a decision on the paper and the authors to improve it

*Please inform the Editor if:*

- There is a conflict of interest
- There is a significant part of the work which you are not able to referee with confidence
- If the work, or a significant part of the work, has previously been published, including online publication (e.g. on a preprint server/open access server)
- You believe the work, or a significant part of the work, is currently submitted elsewhere
- The work represents part of an unduly fragmented investigation

Dalton Transactions Accepted Manuscript

## Graphical Abstract:





Journal Name

COMMUNICATION

## Low-Voltage, High-Brightness and Deep-Red Light-Emitting Electrochemical Cell (LECs) Based on New Ruthenium(II) Phenanthroimidazole Complexes

Received 00th January 20xx,  
Accepted 00th January 20xx

DOI: 10.1039/x0xx00000x

www.rsc.org/

Babak Nemati Bideh,<sup>a</sup> Cristina Roldán-Carmona,<sup>b</sup> Hashem Shahroosvand<sup>a\*</sup> and Mohammad K. Nazeeruddin<sup>b\*</sup>

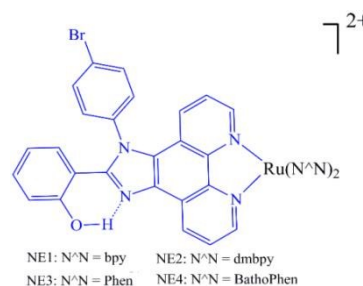
**Light-Emitting Electrochemical Cells (LECs) with a simple device structure ITO/Ru complex/ Ga:In were prepared by using heteroleptic ruthenium(II) complexes containing 2-(2-hydroxyphenyl)-1-(4-bromophenyl)-1H-imidazo [4,5-f] [1,10] phenanthroline (hpbpip) as  $\pi$ -extended ligand. After ancillary ligand modification, [Ru(hpbpip)(dmbpy)<sub>2</sub>] (ClO<sub>4</sub>)<sub>2</sub> complex shows a deep red electroluminescence emission (2250 cd/m<sup>2</sup> at 6 v) centered at 685 nm, 65 nm red-shifted compared to the [Ru(bpy)<sub>3</sub>](ClO<sub>4</sub>)<sub>2</sub> benchmark red-emitter at very low turn voltage (2.6 V), demonstrating its potential for low-cost deep-red light sources. Moreover, the PL quantum yield of [Ru(hpbpip)(bpy)<sub>2</sub>] (ClO<sub>4</sub>)<sub>2</sub> complex revealed higher (0.121) than benchmark standard [Ru(bpy)<sub>3</sub>]<sup>2+</sup> (0.095).**

Light-emitting electrochemical cells (LECs) have attracted much attention in the last few decades as a promising technology for low-cost lighting applications. Compared to other sophisticated technologies such as organic light-emitting diodes (OLEDs), which require multiple evaporation processes and the use of air-sensitive electrodes, LECs exhibit important advantages. In their simplest form they consist of an ionic luminescent material sandwiched between two electrodes,<sup>1</sup> they can be easily processed from solution, and they do not rely on air-sensitive charge-injection layers, avoiding the need of rigorous encapsulation.<sup>2</sup>

The first solid state LECs based on iTMCs were reported in 1996 and utilized an ionic ruthenium polypyridyl complex as light emitting material.<sup>3</sup> Several studies have been carried out in the last decade to enhance the device performance of LECs based on Ru(II) complexes.<sup>4-6</sup> So far [Ru(bpy)<sub>3</sub>]<sup>2+</sup> and its analogues are the most studied ruthenium(II) complexes due to their high<sup>3</sup>MLCT, long excited state lifetimes ( $\tau \approx 1 \mu\text{s}$ ) and luminescence quantum yields ( $\Phi \approx 0.095$ ) in solution at room temperature. [Ru(bpy)<sub>3</sub>]<sup>2+</sup> and its derivatives have already been incorporated in LECs showing high external quantum

efficiencies (EQEs) of up to 6.4%.<sup>5, 7-9</sup> Additionally, phenanthroimidazole derivatives are well known for their extraordinary photophysical properties, thermal stability, and balanced charge transporting capabilities.<sup>10-12</sup> These results suggest that the use of phenanthroimidazole as ligand in ion transition metal complexes could open the way towards new electroluminescent metal complexes for lighting and display applications.

In this paper, a new family of ruthenium complexes of general formula [Ru(N<sup>^</sup>N)<sub>2</sub>(hpbpip)]<sup>2+</sup> (scheme 1) where N<sup>^</sup>N = bipyridine (bpy), 4,4'-Dimethyl-2,2'-dipyridyl (dmbpy), phenanthroline (phen), 4,7-diphenyl-1,10-phenanthroline (bathophen), and hpbpip = 2-(2-Hydroxyphenyl)-1-(4-Bromophenyl)-1H-imidazo[4,5-f][1,10]phenanthroline, a bidentate ligand with an extended aromatic system, was prepared, fully characterized and utilized as emitter in the single layer LEC. We chose hpbpip as ligand because it contains a strong metal-binding 1, 10-phenanthroline heterocycle fused with imidazole, together with its possibility of adjusting the steric and electronic properties of hpbpip by changing the substituents at the N1 and C2 positions of the imidazole.<sup>13, 14</sup>



**Scheme 1.** Phenanthroimidazole-based cationic ruthenium (II) complexes investigated in this work.

Moreover, the large dihedral angle between imidazole and N-Aryl ring suppresses the intermolecular face-to-face  $\pi$ - $\pi$

<sup>a</sup> Chemistry Department, University of Zanjan, Zanjan, Iran.

<sup>b</sup> Group for Molecular Engineering of Functional Materials, Ecole Polytechnique Federale de Lausanne Valais Wallis, Rue de l'Industrie 17, 1950 Sion, Valais, Switzerland

† Electronic Supplementary Information (ESI) available: See DOI: 10.1039/x0xx00000x

Table 1. UV/Vis, Emission, and Redox Properties of NE1-4

Comp.	Absorbance		Emission		Ru(II/III) Oxi.	Ligand Red.	$E_{\text{HOMO}}^f$ (eV)	$E_{\text{LUMO}}^g$ (eV)	$E_{\text{gap}}^h$ (eV)
	$\lambda_{\text{max}}[\text{nm}]$ ( $\log \epsilon$ ) <sup>a</sup>	MLCT	$\lambda_{\text{max}}[\text{nm}]$ ( $\phi$ ) <sup>d</sup>	Solution <sup>b</sup>					
NE1	220 (4.69), 284 (4.97), 323 (4.40)	455 (4.24)	618 (0.121)	626	1.38 (0.070) <sup>i</sup>	-1.020	-5.82	-3.38	2.44
NE2	220 (4.96), 282 (4.94), 318 (4.47)	469 (4.20)	635 (0.096)	676	1.32 (0.060) <sup>i</sup>	-0.880	-5.77	-3.52	2.25
NE3	224 (4.89), 262 (4.97), 337 (4.19)	454 (4.20)	610 (0.086)	626	1.36 (0.105) <sup>j</sup>	-0.860	-5.81	-3.54	2.27
NE4	224 (4.97), 276 (5.10), 329 (4.42)	463 (4.43)	620 (0.078)	635	1.33 (0.126) <sup>j</sup>	-0.960	-5.78	-3.44	2.34
hpbpip	281 (4.9), 322 (4.39), 390 (4.2)	---	480	---	---	---	---	---	---
Ru(bpy) <sub>3</sub> <sup>2+</sup>	245 (4.4), 290 (4.91)	451 (4.17)	621 (0.095)	648	1.29 (0.079) <sup>i</sup>	-1.31 <sup>i</sup>	-5.74	-3.14	2.60

<sup>a</sup> In CH<sub>3</sub>CN solutions (1×10<sup>-5</sup>M). <sup>b</sup> In degassed CH<sub>3</sub>CN solutions at 298 K. <sup>c</sup> Neat films were made on glass substrates with a thickness of about 90 nm. <sup>d</sup> The emission quantum yields were calculated by comparison with [Ru(bpy)<sub>3</sub>]<sup>2+</sup> ( $\phi_{\text{std}} = 0.095$ ) in acetonitrile solution at room temperature. <sup>e</sup> From CV measurements,  $E_{1/2} = 1/2(E_{\text{pa}} + E_{\text{pc}})$ ; 0.1 M acetonitrile/TBAP versus Ag/AgCl. <sup>f</sup> From the formula  $E_{\text{HOMO}} = [-e(E_{\text{ox}} - E_{1/2(\text{Fc}/\text{Fc}^+)})] - 4.8$  eV. <sup>g</sup> From the formula  $E_{\text{LUMO}} = [-e(E_{\text{red}} - E_{1/2(\text{Fc}/\text{Fc}^+)})] - 4.8$  eV. <sup>h</sup> From the formula  $E_{\text{gap}} = E_{\text{HOMO}} - E_{\text{LUMO}}$ . <sup>i</sup> An reversible electrochemical process. <sup>j</sup> A quasi-irreversible electrochemical process. <sup>k</sup> An irreversible electrochemical process.

stacking of these complexes through hpbpip in the solid state (ESI, Fig. S6) and thus, it prevents self-quenching of emission.<sup>15</sup>

The full synthesis processes as well as the characterization of the four Ruthenium complexes are reported in the S.I.

The absorption spectra of the Ru(II) complexes are shown in Figure 1 and the energy maxima and absorption coefficients are summarized in Table 1. The lowest-energy absorption band is located around 460 nm and can be attributed to a spin-allowed metal-to-ligand charge-transfer (MLCT) transition due to an overlapping of  $d\pi(\text{Ru}) \rightarrow \pi^*(\text{bpy or phen})$  and  $d\pi(\text{Ru}) \rightarrow \pi^*(\text{hpbpip})$  transitions. The intense intraligand band around 275 nm originates from a polypyridyl transition  $\pi \rightarrow \pi^*$ .<sup>16</sup> The smaller bands around 330 nm are attributed to intraligand bands from the phenanthroimidazole ligand.<sup>17</sup>

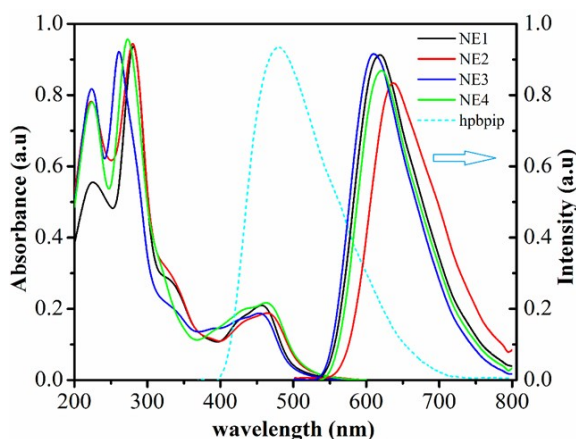


Figure 1. Electronic absorption and emission spectra of NE1-4

The MLCT absorption maximum of complexes is red-shifted by about 5 to 14 nm compared with that of [Ru(bpy)<sub>3</sub>]<sup>2+</sup> because phenanthroimidazole ligands have larger extent of  $\pi$  delocalization. Furthermore, the MLCT band of NE2 (469 nm) and NE4 (463 nm) complexes is bathochromically shifted relative to those of NE1 (455 nm) and NE3 (454 nm), respectively.

The photoluminescence obtained for all the complexes and hpbpip in deoxygenated acetonitrile and chloroform, respectively, are presented in Fig. 1. As can be observed, the NE1 complex exhibits a photoluminescence quantum yield (QY) significantly higher compared with the reference complex [Ru(bpy)<sub>3</sub>]<sup>2+</sup> and its analogues (see Table 1) demonstrating the beneficial effect of incorporating hpbpip-ligand in [Ru(bpy)<sub>3</sub>]<sup>2+</sup>. Interestingly, the maximum emission of NE2 is red-shifted relative to the other complexes, exhibiting  $\lambda_{\text{max}} \sim 635$  nm. A similar trend is observed when the complexes are embedded in a thin solid film (ESI, Fig. S7). The emission maxima of the pure thin film of complexes are shifted to lower energies, respect to the solution, due to the influence of the environment that attributed to polarity effects of the medium of the luminescent complexes.<sup>6, 18, 19</sup> NE1, NE3 and NE4 shows a red shift of about 8 to 15 nm relative to the PL spectra in solution. Nevertheless the most affected emission is observed for the complex NE2, where 40 nm of  $\lambda_{\text{max}}$  displacement was measured probably due to the aggregation in solid film.

The ligand strategy is based on excited state intramolecular proton transfer (ESIPT). This is a four-level photocycle process involving enol (E) to keto (K) phototautomerization ( $E \rightarrow E^* \rightarrow K^* \rightarrow K \rightarrow E$ ). ESI. Fig. S8).<sup>20</sup> The existence of intramolecular hydrogen bond in hpbpip is

confirmed by the presence of the singlet at 13.17 ppm in the  $^1\text{H}$ NMR spectra, which is a typical signal for hydrogen bonded hydrogen atom (ESI, Fig. S1). The intramolecular hydrogen bonding, which is the driving force for ESIPT, has a significant effect on the optical properties of hbbpip and their derivatives, as it prevents the rotation of the benzene ring and decreases the self-quenching.<sup>15,21</sup> As a consequence, this process leads to a large Stokes-shifted luminescence from the keto-form which offers an advantage by minimizing the self-absorption.<sup>22</sup> A fluorescence peak with emission centered at 480 nm is also detected for hbbpip and assigned to a rotamer keto form (Fig. 1). In addition to, the ESIPT process enhances the fluorescence emission, can be applied in the solid state ESIPT emitters.<sup>22</sup>

Density functional theory (DFT) calculations were carried out and the electronic structure and localization of the frontier orbitals of ruthenium(II) complexes are illustrated in Figure S10. For all complexes, the highest-occupied molecular orbitals (HOMOs) are localized on the hydroxy phenyl and imidazole fused ring of phenanthroimidazole ligand and the lowest-unoccupied molecular orbitals (LUMOs) are located on the other

polypyridyl ligand and some on the phenanthroline moiety of hbbpip ligand. Also, DFT calculations show that the phenanthroimidazole ligand possesses a larger dihedral angle with the imidazole and bromophenyl ring ( $89^\circ$ ), whereas, the fused core of it is planar. In addition the large dihedral angle between them suppresses the intermolecular  $\pi$ - $\pi$  stacking in the solid state and prevents self-quenching of emission intensity (ESI, Fig. S6). Localization of the frontier orbitals of these complexes are compared with archetypal Ir-ITMC as most popular complex in the LEC applications. In this aspect, role of hbbpip ligand in these complexes is similar to the cationic cyclometalated ligand in iridium complex such as  $[(ppy)_2Ir(bpy)]^+$ .

The electrochemical properties of phenanthroimidazole ligand based ruthenium(II) complexes were studied with cyclic voltammetry (CV) measurements (Fig. 2). The cyclic voltammograms of these four Ru(II) complexes exhibit four or three successive waves attributed to one metal-centered oxidation and three or two ligand-based reductions. According to the peak to peak separation, the oxidation

**Table 2.** Electrical characteristics of ITO/[Ru(N<sup>^</sup>N)<sub>2</sub>(hbbpip)]<sup>2+</sup> / Ga: In /epoxy LEC Devices

Complexes	$\lambda_{\text{max}}$ [nm]	CIE <sup>a</sup> [x, y]	FWHM [nm]	$J_{\text{max}}$ <sup>b</sup>	$t_{\text{on}}$ <sup>c</sup>	$L_{\text{max}}$ <sup>d</sup>	$R^e$ [W]	EQE <sup>f</sup>
NE1	633	[0.652,0.315]	155	2020	2.8	1500	$5 \times 10^{-5}$	0.53
NE2	685	[0.662, 0.316]	153	2100	2.6	2250	$10^{-4}$	0.61
NE3	660	[0.690, 0.305]	168	2200	2.7	790	$3 \times 10^{-5}$	0.24
NE4	662	[0.630, 0.308]	156	1790	3.3	1125	$2 \times 10^{-5}$	0.33
[Ru(bpy) <sub>3</sub> ] <sup>2+</sup>	632	[0.693, 0.308]	137	2910	2.3	2500	-	0.65

<sup>a</sup> CIE(x,y): Commission Internationale de l'Éclairage, being the D65 white reference CIE<sub>(x,y)</sub> = (0.31;0,33). <sup>b</sup> Maximum current density [A  $\cdot$  m<sup>-2</sup>] at 5 V. <sup>c</sup> Turn-on voltage [V]. <sup>d</sup> Maximum luminance [cd m<sup>-2</sup>]. <sup>e</sup> Maximum light output [W]. <sup>f</sup> external quantum efficiency [%].

(Ru<sup>II,III</sup> redox couple) part of these complexes exhibited one nearly reversible wave for NE1 and NE2 and quasi-reversible wave for other complexes. The electron abstraction from the metal center is more difficult in NE1 ( $E_a = 1.42$  V), than it is from [Ru(bpy)<sub>3</sub>]<sup>2+</sup> ( $E_a = 1.33$  V). Furthermore, the first reduction value -1.02 V is significantly anodically shifted with respect to that of [Ru(bpy)<sub>3</sub>]<sup>2+</sup> (-1.31 V), which stresses the better  $\pi$ -electron acceptor character of the phenanthroimidazole ligand (hbbpip) contained in complex NE1. Interestingly, the sequential substitution of bpy in [Ru(bpy)<sub>3</sub>]<sup>2+</sup> with hbbpip increases the oxidation potential of ruthenium steadily, resulting in an overall anodic shift of 90 mV for [Ru(bpy)<sub>2</sub>(hbbpip)]<sup>2+</sup> (NE1) compared to [Ru(bpy)<sub>3</sub>]<sup>2+</sup>. The HOMO and LUMO energy levels and hence the energy gap, of the complexes were calculated using the empirical relations (ESI) as shown in Table 1. The band gap of these complexes follow the order NE1>NE4>NE3>NE2 (ESI, Fig. S9). Finally, complexes NE1–4 were employed as the electroluminescent materials in single-layer LECs and their electroluminescence (EL) properties were evaluated. The device architecture employed for the preparation of the cells is based on a thin ITMC-layer (~85 nm) sandwiched between ITO and Ga:In electrode.

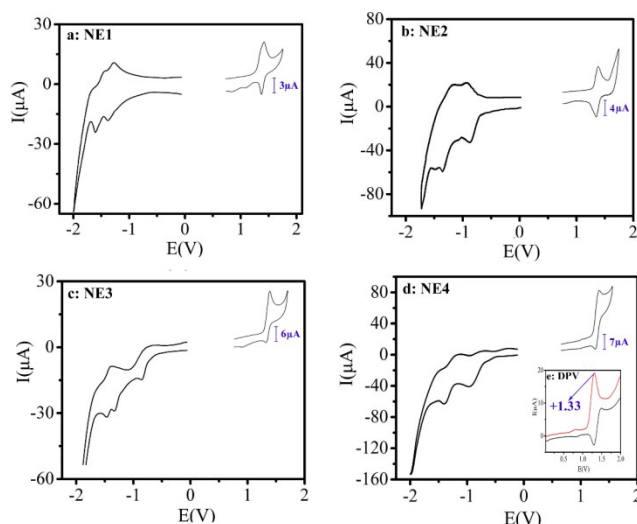


**Figure 2.** Cyclic voltammograms of complexes NE1–4.

The key parameters that represent the performances of LECs are summarized in Table 2. It can be observed that NE2 has the highest luminance and efficacy, together with the lowest turn on voltage among all the investigated complexes. Upon applying a bias of 3 V to the device, the current density rapidly

increases with time and bright red emission is clearly observed, as typically occurs in LECs, see Fig 4. As can be observed in figure 3, NE1 and NE2 present the highest and lowest EL maxima respectively, with  $\lambda_{\max}$  values of 633 and 685 nm. Meanwhile, NE3 and NE4 exhibit similar EL spectra centered at 660 and 662 nm respectively, accompanied by analogous pattern in phenanthroline ancillary ligand.<sup>10, 23a</sup> These strong red-shift in EL and PL of thin film respect to the PL of solution is related to a change in the film composition in the solid state and the manner of excitation used. This behavior has already been observed in other LEC devices and was said to be related to a change of emissive excited state in the solid state.<sup>22b</sup> Under high electrical fields in LEC devices, the molecular orbitals of the ionic complex might be polarized and, thus, the energy level would decrease, resulting in the red-shift of EL spectrum respect to the PL of thin film.<sup>23c</sup> For the NE3 and NE4 molecules, the devices showed a moderate red-shifted emission ( $\sim 30$  nm), while in the case of NE2 it was more significant ( $>50$  nm) compared to  $[\text{Ru}(\text{bpy})_3]^{2+}$  as a benchmark emitter. As a result, the Commission Internationale de L'Éclairage (CIE) color coordinates of NE2 presented a deep-red color, with CIE(x,y) coordinates equal to (0.654, 0.344). It is worth to notice that the maximum luminance ( $L_{\max}$ ) obtained for the devices using complexes NE 1-4 are above those previously reported for similar phenanthroline complexes (see Fig. 4).<sup>10, 23, 24</sup> Moreover, the luminance of NE2 is also comparable to the reported luminance for LEC based on benchmark  $[\text{Ru}(\text{bpy})_3]^{2+}$ . A possible reason for explaining this behavior is based on the insertion of Methyl group on the positions 4, 4' of bpy ligand (device NE2), which strongly improves the device characteristics due to the increase of donor ligands compared to other derivatives.<sup>25</sup>

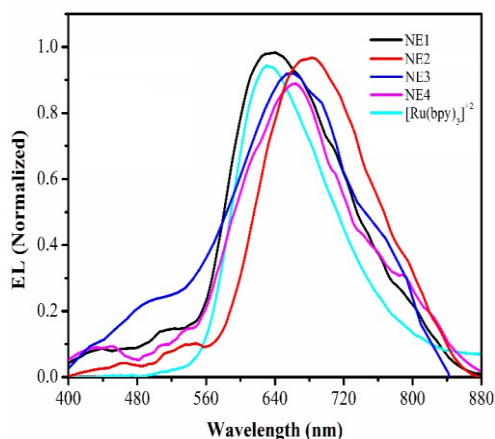


**Figure 3.** EL spectra of NE1-4 and  $[\text{Ru}(\text{bpy})_3](\text{ClO}_4)_2$ .

According to the electrochemical data, the phenanthroimidazole ligand shows better  $\pi$ -electron acceptor character compared with bipyridine, which lowers the energy of the  $^3\text{MLCT}$  state. Additionally, the electron-donating methyl group increases the energy of the  $^3\text{MC}$  state, thus reducing radiationless deactivation via the latter state and enhancing the excited state lifetime and luminescence in NE2 complex. This pull-push system shifts the emission energy of NE2 to lower energy in the EL and PL spectrum.<sup>9</sup> As a consequence, the designed molecular structure leads to a large improvement in the device performance, presenting instantaneous and bright electroluminescence ( $L_{\max} = 2250 \text{ cd.m}^{-2}$ ), deep-red

emission (685 nm) and a low turn-on voltage of 2.6 V, indicating a very efficient charge injection in the Ru(II)-polypyridyl complexes. The light output (R/W) obtained for the LEC devices using NE1-4 at an applied bias of 6V is depicted in Figure 5. Maximum light outputs around  $10^{-4} \text{ W}$  are reached after approximately 12 minutes for the devices using complex NE2 respectively (Fig. 5). These values are among the highest reported for LEC devices based on charged ruthenium polypyridyl complexes emitting in the deep-red regions. We attribute this improvement to the combination of two effects: (i) the high PL quantum yield, which increases the radiative recombination, and (ii) the high mobility of the counter ion  $\text{ClO}_4^-$ , which is fast enough to attain a steady state within a reasonable time<sup>26</sup>. The values of the external quantum efficiency (EQE) for the LECs are shown in Table 2. LEC devices fabricated with the NE2 complex exhibit a higher EQE than LECs based on NE1 and other complexes. This demonstrates the positive effect of methyl as donor substitution on the bpy ligand in the NE2 complex on the device performance. Another striking feature is the low turn on voltage observed for the devices. In LECs, the counter ions of iTMC plays a key role in promoting the charge injection from the cathode electrode, as well as stabilizing the electron and hole transport through the device. In the presented  $[\text{Ru}(\text{N}^{\wedge}\text{N})_2(\text{hpbpip})]^{2+}$  based devices, when applying a bias,  $\text{ClO}_4^-$  and  $[\text{Ru}(\text{N}^{\wedge}\text{N})_2(\text{hpbpip})]^{2+}$  ions drift through the electrodes leading to the accumulation of negative charge near the anode interface and positive charge at the cathode interface (ESI, Fig. S. 11).

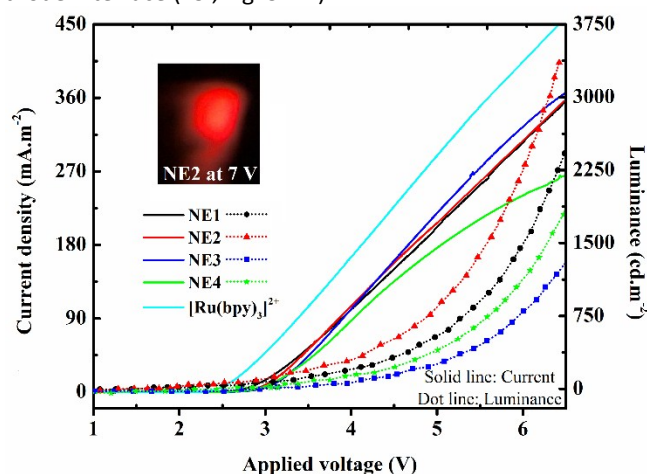


**Figure 4.** Current density and Luminance as a function of voltage for NE1-4 devices. Inset: Photograph showing deep red emission of a single-layer LEC ITO/NE2/Ga:In at applied voltage 7 V.

With increasing voltage the accumulation of ions along the electrodes increases and the barrier energy for the injection decreases,<sup>27</sup> detecting higher current density. In our system, the holes are stabilized by the displaced  $\text{ClO}_4^-$  ions, while electrons are injected from the cathode into the  $t_{2g}^*$  orbital of the  $\text{Ru}^{2+}$ .<sup>28</sup>

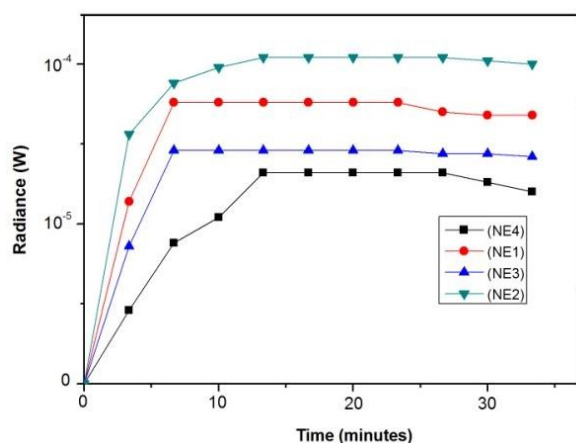


**Figure 5.** Radiant flux vs time for ITO/[NE1-4]/Ga:In devices.

Summary, by chemically modifying the  $[\text{Ru}(\text{N}^{\wedge}\text{N})_2(\text{hpbpip})]^{2+}$  complex, the maximum luminance of the resulting devices was increased to a value as high as  $3000 \text{ cd. m}^{-2}$  at 7 V. This value represents a performance that not only is comparable to the established  $[\text{Ru}(\text{bpy})_3]^{2+}$  emitter but also corresponds to a deeper red emission centered at 685 nm with very low turn on voltage (2.6 V). All these properties converts  $[\text{Ru}(\text{N}^{\wedge}\text{N})_2(\text{hpbpip})]^{2+}$  complexes in very attractive candidates for the preparation of bright, low turn-on voltage and deep-red light-emitting electrochemical cells, which represent a potential route for simple low-cost lighting sources.

## Notes and references

- Q. B. Pei, G. Yu, C. Zhang, Y. Yang and A. J. Heeger, *Science*, 1995, **269**, 1086.
- R. D. Costa, E. Ortí, H. J. Bolink, F. Monti, G. Accorsi and N. Armadori, *Angew. Chem., Int. Ed.*, 2012, **51**, 8178.
- J. K. Lee, D. S. Yoo, E. S. Handy and M. F. Rubner, *M. F., Appl. Phys. Lett.* 1996, **69**, 1686.
- J. Slinker, D. Bernards, P. L. Houston, H. D. Abruna, S. Bernhard and G. G. Malliaras, *G. G., Chem. Commun.* 2003, 2392.
- G. Kalyuzhny, M. Buda, J. McNeill, P. Barbara, and A. J. Bard, *J. Am. Chem. Soc.* 2003, **125**, 6272.
- H. J. Bolink, L. Cappelli, E. Coronado and P. Gavina, *Inorg. Chem.* 2005, **44**, 5966.
- C.-Y. Liu, and A. J. Bard, *Appl. Phys. Lett.* 2005, **87**, 061110.
- S. Xun, J. Zhang, X. Li, D. Ma, and Z. Wang, *Synth. Met.* 2008, **158**, 484.
- A. Breivogel, M. Park, D. Lee, S. Klassen, A. Kühnle, C. Lee, K. Char, and K. Heinze, *Eur. J. Inorg. Chem.* 2014, 288.
- P. Dreyse, B. Loeb, M. Soto-Arriaza, D. Tordera, E. Ortí, J. J. Serrano-Pérez, and H. J. Bolink, *Dalton Trans.*, 2013, **42**, 15502.
- Y. Yuan, J.-X. Chen, F. Lu, Q.-X. Tong, Q.-D. Yang, H.-W. Mo, T.-W. Ng, F.-L. Wong, Z.-Q. Guo, J. Ye, Z. Chen, X.-H. Zhang, and C.-S. Lee, *Chem. Mater.* 2013, **25**, 4957.
- Z. Wang, P. Lu, S. Chen, Z. Gao, F. Shen, W. Zhang, Y. Xu, H. S. Kwok and Y. Ma, *J. Mater. Chem.* 2011, **21**, 5451.
- S. Rosepriya, A. Thiruvalluvar, J. Jayabharathi, M. V. Perumal, R. J. Butcher, J. P. Jasinski and J. A. Golen, *Acta Crystallogr. E*, 2011, **67**, 0989
- Q. Zhao, S. Liu, M. Shi, F. Li, H. Jing, T. Yi and C. Huang, *Organometallics*, 2007, **26**, 5922; J. Sun, W. Wu, H. Guo and J. Zhao, *Eur. J. Inorg. Chem.*, 2011, 3165
- Z. Wang, Y. Feng, H. Li, Z. Gao, X. Zhang, P. Lu, P. Chen, Y. Ma and S. Liu, *Phys. Chem. Chem. Phys.* 2014, **16**, 10837.
- E. R. Holmlin, J. A. Yao and J. K. Barton, *Inorg. Chem.* 1999, **38**, 174.
- B. W. Jing, M. H. Zhang and T. Shen, *Spectrochim. Acta, Part A*. 2004, **60**, 2635.
- (a) S. Evariste, M. Sandroni, T. W. Rees, C. Roldán-Carmona, L. Gil-Escrig, H. J. Bolink, E. Baranoff and E. Zysman-Colman, *J. Mater. Chem. C*, 2014, **2**, 5793 (b) J. D. Slinker, A. A. Gorodetsky, M. S. Lowry, J. Wang, S. Parker, R. Rohl, S. Bernhard and G. G. Malliaras, *J. Am. Chem. Soc.*, 2004, **126**, 2763.
- H. J. Bolink, L. Cappelli, E. Coronado, M. Grätzel, and Md. K. Nazeeruddin, *J. Am. Chem. Soc.*, 2006, **128**, 46.
- J. E. Kwon and S. Y. Park, *Adv. Mater.* 2011, **23**, 3615; C. Fang, R. R. Frontiera, R. Tran and R. A. Mathies, *Nature*, 2009, **462**, 200.
- J. E. Kwon, S. Park, S. Y. Park, *J. Am. Chem. Soc.* 2013, **135**, 11239; Y. Houari, S. Chibani, D. Jacquemin and A. D. Laurent, *J. Phys. Chem. B*, 2015, **119**, 2180.
- V. S. Padalkar and S. Seki, *Chem. Soc. Rev.*, 2016, **45**, 169.
- (a) D. Tordera, A. Pertegas, N. M. Shavaleev, R. Scopelliti, E. Ortí, H. J. Bolink, E. Baranoff, M. Grätzel and M. K. Nazeeruddin, *J. Mater. Chem.*, 2012, **22**, 19264 (b) H. J. Bolink, L. Cappelli, S. Cheylan, E. Coronado, R. D. Costa, N. Lardiés, Md. K. Nazeeruddin and E. Ortí, *J. Mater. Chem.*, 2007, **17**, 5032 (c) Y. M. Wang, F. Teng, Y. B. Hou, Z. Xu, Y. S. Wang, W. F. Fu, *Appl. Phys. Lett.* 2005, **87**, 233512.
- C. D. Sunesh, G. Mathai and Y. Choe, *ACS Appl. Mater. Interfaces* 2014, **6**, 17416.
- E. S. Handy, A. J. Pal and M. Rubner, *J. Am. Chem. Soc.* 1999, **121**, 3525; Y. Chuai, D. N. Lee, N. Zhen, J. H. Min, B. H. Kim and D. Zou, *Syn. Met.* 2004, **145**, 259.
- M. Buda, G. Kalyuzhny, A. J. Bard, *J. Am. Chem. Soc.* 2002, **124**, 6090.
- F. F. Fan and A. J. Bard, *J. Phys. Chem. B* 2003, **107**, 1781; C. Zhen, Y. Chuai, C. Lao, L. Huang, D. Zou, D. N. Lee and B. H. Kim, *Appl. Phys. Lett.*, 2005, 093508.
- T. D. Shoji, Z. Zhu and J. M. Leger, *ACS Appl. Mater. Interfaces* 2013, **5**, 11509.